Preparation and Structural Characterization of $[K(18\text{-crown-6})]^+$ Salts of $[RNSN]^-$ Anions and the $[NSN]^{2-}$ Dianion

Tobias Borrmann,[a] Enno Lork,[b] Rüdiger Mews,*[b] Makhmut M. Shakirov,[c] and Andrey V. Zibarev*[c]

Keywords: Sulfur / Nitrogen / X-ray diffraction / NMR spectroscopy

$[K(18\text{-crown-6})]^+$ salts of the $[RNSN]^-$ anions (R = Alk, Ar) and the $[NSN]^{2-}$ dianion, which are thermally stable and very soluble in aprotic organic solvents, were prepared from $[K(18\text{-crown-6})]^+[t\text{BuO}]^-$ and the corresponding R–N=S=N–$SiMe_3$ and $(Me_3Si–N=)_2S$, respectively. The salts are characterized by multinuclear (^1H, ^{13}C, ^{14}N, ^{19}F, ^{29}Si and ^{39}K) NMR spectroscopy in solution and by X-ray diffraction in the solid state. The experimentally determined bond lengths confirm that the $[RNSN]^-$ anions are thiazylamides, $R–N^––S{\equiv}N$ rather than sulfur diimides, $R–N=S=N^–$. Relative to O=S=O, in the $[NSN]^{2-}$ dianion, which is the genuine aza-analogue of sulfur dioxide, the bond lengths are elongated and the bond angle is widened. This might reflect electrostatic repulsion between the negatively charged N atoms. The experimental results are in agreement with theoretical calculations (RHF, B3LYP, MP2). In the nitrogen NMR spectra, when going from $[AlkNSN]^-$ to $[ArNSN]^-$, the low-field signal of the terminal (unsubstituted) N atom reveals further deshielding, whereas the high-field signal of the internal (substituted) N atom displays further shielding. The ^{14}N NMR resonance for the $[NSN]^{2-}$ dianion is practically insensitive to the counterion.

Introduction

Although known for more than 50 years, the sulfur-nitrogen triple bond still belongs to the less studied multiple bonds. Only relatively few thiazyne derivatives, $R-S{\equiv}N$ and $R_3S{\equiv}N$, are unambiguously characterized, either because of their thermal instability or because of the lack of generally applicable synthetic routes.[1–5]

Recently, it was shown by low-temperature X-ray crystallography and non-empirical calculations at the MP2 and B3LYP levels of theory that $[RNSN]^-$ anions (R = Alk, Ar), which are easily accessible by the fluoride ion-induced desilylation of $R-N=S=N-SiMe_3$ precursors (Scheme 1), should be regarded as thiazylamides $R-N^–-S{\equiv}N$ rather than the expected sulfur diimides $R-N=S=N^–$.[6–8]

Besides their theoretical importance, the $[RNSN]^-$ anions and the related $[NSN]^{2-}$ dianion are also of practical interest for synthetic chemistry as key intermediates for various inter- and intramolecular condensations[9–19] They can also be used as ligands for coordination compounds.[20] The anions are also useful for the solving of some problems of molecular physics related to intramolecular electron-transfer processes,[21] and are worthy of investigation as potential components of molecular conductors based on radical-ion salts.[22]

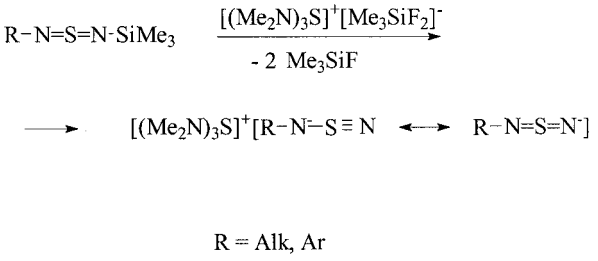

Scheme 1

Previously, the $[RNSN]^-$ anions were isolated and structurally characterized in the form of air-sensitive and thermally unstable salts of the tris(dimethylamino)sulfonium (TAS^+) cation (Scheme 1),[6–8] which decompose above about −20 °C, especially when R = Ar. Such instability seriously complicates further investigations and applications of the $[RNSN]^-$ anions.

On the other hand, the potassium salts of the $[RNSN]^-$ anions (where R = *t*Bu, Me_3Si) and of the $[NSN]^{2-}$ di

[a] Institute of Organic Chemistry, NW2 C, University of Bremen, 28334 Bremen, Germany
[b] Institute for Inorganic and Physical Chemistry, NW2 C, University of Bremen,
28334 Bremen, Germany
Fax: (internat.) + 49-421-218-4267
E-mail: mews@chemie.uni-bremen.de
[c] Institute of Organic Chemistry, Russian Academy of Sciences, 630090 Novosibirsk, Russia
Fax: (internat.) + 7-3832-344-752
E-mail: zibarev@nioch.nsc.ru

  DOI: 10.1002/ejic.200300954

anion, in particular those prepared by the N−Si bond cleavage of the corresponding R−N=S=N−$SiMe_3$ precursors with *t*BuOK, are thermally very stable. They are almost insoluble in common aprotic solvents due to strong anion−cation interaction.[17,23,24] As a consequence, these salts have never been structurally characterized because they were not obtained as single crystals suitable for X-ray crystallography.

This article describes the preparation and isolation of the thermally stable [K(18-crown-6)]$^+$ salts of the [RNSN]$^-$ anions (R = Alk, Ar) and of the [NSN]$^{2-}$ dianion, which are readily soluble in organic solvents. The salts have been characterized by X-ray diffraction and by multinuclear (^{1}H, ^{13}C, ^{14}N, ^{19}F, ^{29}Si and ^{39}K) NMR spectroscopy in solution.

Results and Discussion

As mentioned above, K^+ salts of the [RNSN]$^-$ anions (R = *t*Bu, Me_3Si) and the [NSN]$^{2-}$ dianion were obtained previously by the action of *t*BuOK (and also KNH_2) on the R−N=S=N−$SiMe_3$ or $(Me_3SiN=)_2S$ sulfur diimides, respectively.[17,23,24] However, for these salts strong anion−cation interaction resulted in extremely low volatility (not sublimable) and solubility in organic solvents (not crystallizable), which complicated their further purification and unambiguous structural characterization.

The reaction of the R−N=S=N−$SiMe_3$ (R = Alk, Ar) and $(Me_3SiN=)_2S$ precursors with [K(18-crown-6)]$^+$ [*t*BuO]$^-$ under very mild conditions (at −30 °C in THF) has been used as a nearly quantitative general approach to the organic solvent-soluble salts **1**−**6** with the [RNSN]$^-$ anions and the [NSN]$^{2-}$ dianion (Scheme 2). The *t*Bu−O−$SiMe_3$ by-product (liquid, b. p. 102−103 °C) is inert under these reaction conditions and does not interfere with the isolation of the target salts.

$$R-N{=}S{=}N-SiMe_3 + [K(18\text{-crown-}6)]^+[t\text{BuO}]^- \longrightarrow [K(18\text{-crown-}6)]^+[RNSN]^- + t\text{BuOSiMe}_3$$

R = 1-Ad (**1**), *t*Bu (**2**), Me_3Si (**3**), Ph (**4**), 4-FC_6H_4 (**5**)

$$Me_3Si-N{=}S{=}N-SiMe_3 + 2[K(18\text{-crown-}6)]^+[t\text{BuO}]^- \longrightarrow \{[K(18\text{-crown-}6)]^+\}_2[NSN]^{2-} + 2\ t\text{BuOSiMe}_3$$

6

Scheme 2

The salts **1**−**6** (Scheme 2) are thermally very stable. They decompose (depending on R) in the range of approximately 100 °C (**5**) to approximately 150 °C (**2**, **6**) (see Exp. Sect. for details).

Importantly, by using this approach, it was possible to obtain the salts of interest in the form of single crystals suitable for X-ray crystallography using low-temperature crystallization from organic solvents. The solid-state structures of the salts **1** and **3**−**6** are shown in Figure 1 and Figures 2−5, respectively, and the details of the structure

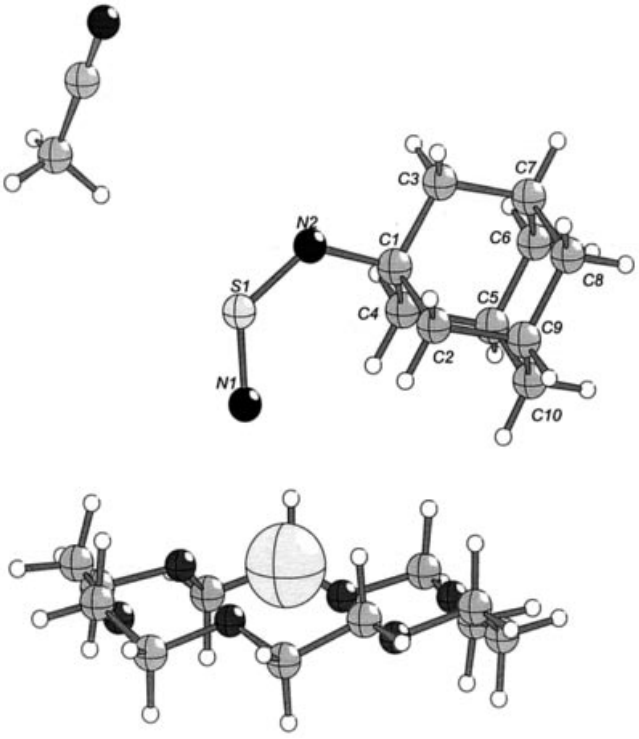

Figure 1. X-ray structure of [K(18-crown-6)]$^+$[1-AdNSN]$^-$·MeCN (**1**)

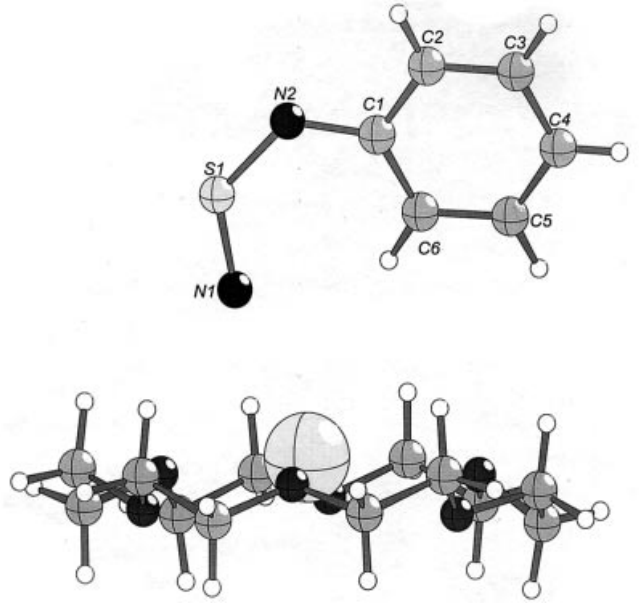

Figure 2. X-ray structure of [K(18-crown-6)]$^+$[PhNSN]$^-$ (**4**)

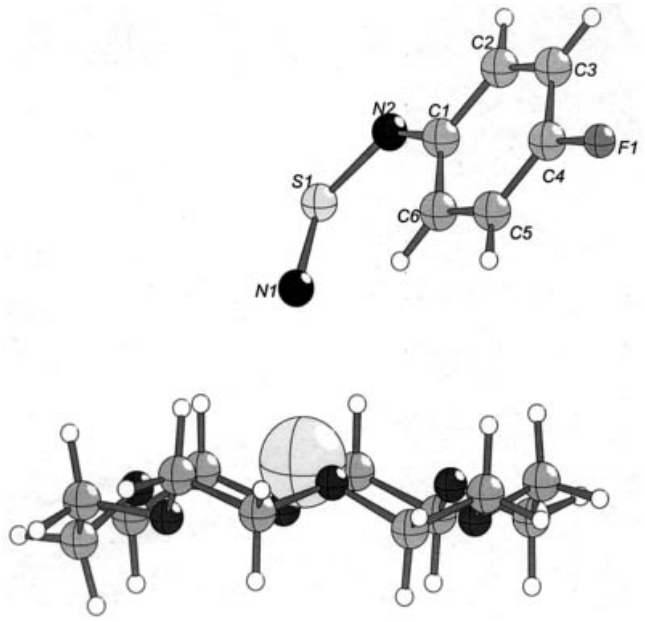

Figure 3. X-ray structure of $[K(18\text{-crown-6})]^+[4\text{-}FC_6H_4NSN]^-$ (**5**)

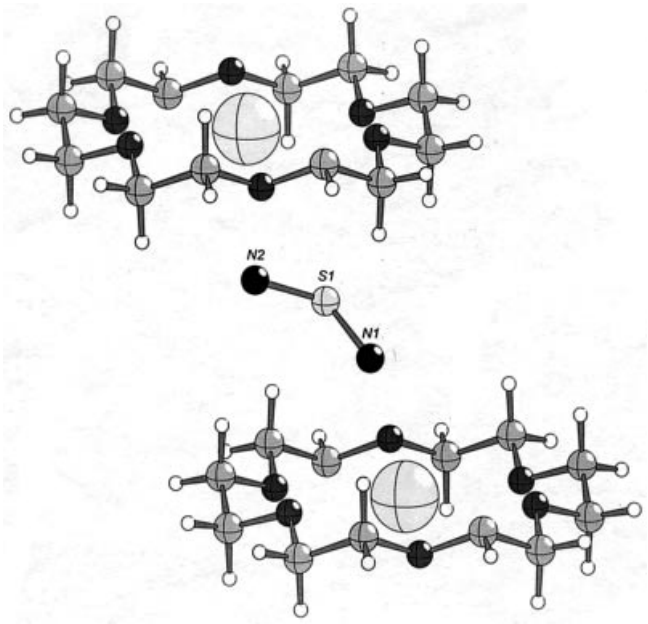

Figure 5. X-ray structure of $\{[K(18\text{-crown-6})]^+\}_2[NSN]^{2-}$ (**6**)

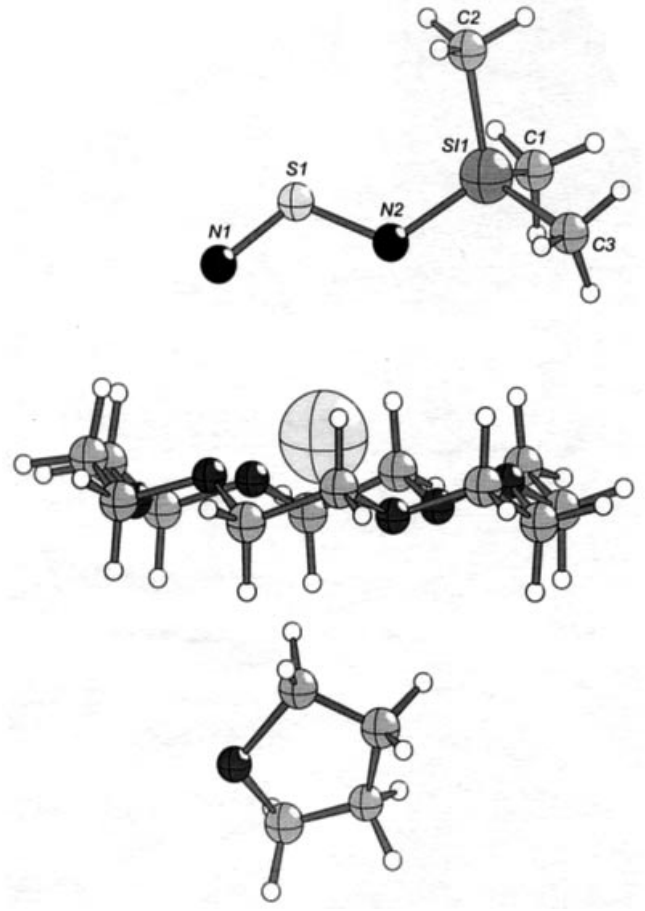

Figure 4. X-ray structure of $[K(18\text{-crown-6})]^+[Me_3SiNSN]^-$ (**3**)

determinations are listed in Table 1. Selected bond lengths and bond angles are given in Table 2. The structures of the $[PhNSN]^-$ anion (salt **4**), the parent anion of the $[ArNSN]^-$ family,[6,8] and the $[NSN]^{2-}$ dianion (salt **6**) are described for the first time. The X-ray structure of salt **2** was not solved due to strong disorder of both cation and anion, but this salt was unambiguously characterized in solution by multinuclear NMR spectroscopy (see below).

In the solid state, all $[RNSN]^-$ anions with R = 1-Ad, Ph, $4\text{-}FC_6H_4$ (salts **1**, **4**, **5**) exhibit the expected *Z*-configuration (Figure 1, Figure 2, Figure 3), whereas the $[Me_3SiNSN]^-$ anion (salt **3**) demonstrates the stereoelectronically unfavorable *E*-configuration (Figure 4), previously also observed for its TAS^+ salt (for the in-depth discussion of the *Z*- and *E*-configurations and the bonding properties of the $[RNSN]^-$ anions, see refs.[7,8]). In the salts with the anions in the *Z*-configuration, the K^+ counterion (encapsulated in the crown ether) is coordinated only by the terminal nitrogen atom (Figure 1, Figure 2, Figure 3), whereas the K^+ cation interacts with the anion in the *E*-configuration symmetrically with both the terminal and the internal N atoms (Figure 4). Due to this coordination the N−S−N bond angle in the $[Me_3SiNSN]^-$ anion is significantly narrower than in the other $[RNSN]^-$ anions (Table 2). In all cases, the N···K^+ separation in these salts (Table 2) is shorter than the sum of van der Waals radius of the N atom (150 pm) and the ionic radius of K^+ (157 and 164 pm for coordination numbers 8 and 12, respectively),[25] which implies relatively strong anion−cation interaction. Interestingly, for salt **3** the S···K^+ distance (Table 2) is rather close to the sum of the van der Waals radius of S (185 pm) and ionic radius of K^+.

Experimentally determined bond lengths (Table 2) confirm that the $[RNSN]^-$ anions should be described as thiazyl anions R−N^-−S≡N rather than sulfur diimide anions R−N=S=N^-. In the anions studied (Table 2), both the sulfur−nitrogen bonds are very different. While the terminal sulfur−nitrogen bond length falls into the range established for the S^{IV}≡N triple bond (146−148 pm), the internal sulfur−nitrogen bond is 9−13 pm longer (Table 2). Comparing the TAS^+ and $[K(18\text{-crown-6})]^+$ salts of the

Table 1. Crystal data and structure refinement for the salts **1** and **3**−**6**

Salt	**1**	**3**	**4**	**5**	**6**
Empirical formula	$C_{22}H_{39}KN_2O_6S{\cdot}C_2H_3N$	$C_{15}H_{33}KN_2O_6SSi{\cdot}C_4H_8O$	$C_{18}H_{29}KN_2O_6S$	$C_{18}H_{28}FKN_2O_6S$	$C_{12}H_{24}KN_2O_6S$
Molecular mass	539.77	508.79	440.59	458.58	363.49
Temperature, K	173(2)	173(2)	173(2)	173(2)	173(2)
Wavelength, pm	71.073	71.073	71.073	71.073	71.073
Crystal system	orthorhombic	orthorhombic	triclinic	triclinic	monoclinic
Space group	*P*na2$_1$	$P2_12_12_1$	*P*1	$P\bar{1}$	$P2_1/c$
a, pm	1706.5(3)	943.85(19)	848.79(17)	989.5(2)	780.2(2)
b, pm	1519.6(3)	1408.8(3)	854.42(17)	991.1(2)	1490.9(2)
c, pm	1105.3(2)	2103.6(4)	881.42(18)	1398.1(3)	773.0(2)
α (°)	90	90	74.65(3)	94.20(3)	90
β (°)	90	90	69.36(3)	109.11(3)	99.85(2)
γ (°)	90	90	70.72(3)	114.95(3)	90
Volume, nm^3	2.8662(10)	2.7972(10)	0.55663(19)	1.1382(4)	0.8859(3)
Z	4	4	1	2	2
$D_{calcd.}$, Mg·m^{-3}	1.251	1.208	1.314	1.338	1.363
Absorption coefficient (mm^{-1})	0.298	0.344	0.367	0.368	0.445
Crystal size (mm^3)	0.50 × 0.40 × 0.40	0.50 × 0.40 × 0.30	0.50 × 0.40 × 0.40	0.40 × 0.25 × 0.20	0.70 × 0.50 × 0.40
θ range for data collection (°)	2.39−26.00	2.42−26.12	2.56−26.09	2.34−21.50	2.65−27.50
Reflections collected	39201	39199	7867	6246	8000
Independent reflections	5563 [*R*(int) = 0.0676]	5508 [*R*(int) = 0.0740]	4019 [*R*(int) = 0.0338]	2498 [*R*(int) = 0.0942]	2023 [*R*(int) = 0.0625]
Completeness to θ, % (θ°)	98.9 (26.00)	98.9 (26.12)	91.0 (26.09)	95.6 (21.50)	100.0 (27.50)
Data/restraints/parameters	5563/1/321	5508/0/286	4019/3/256	2498/0/264	2023/1/199
Goodness-of-fit on F^2	0.946	0.975	1.006	0.703	1.093
Final *R* indices [$I > 2\sigma(I)$]	*R*1 = 0.0395, *wR*2 = 0.0923	*R*1 = 0.0480, *wR*2 = 0.1225	*R*1 = 0.0308, *wR*2 = 0.0732	*R*1 = 0.0411, *wR*2 = 0.0571	*R*1 = 0.0345. *wR*2 = 0.0878
R indices (all data)	*R*1 = 0.0521, *wR*2 = 0.0963	*R*1 = 0.0617, *wR*2 = 0.1304	*R*1 = 0.0337, *wR*2 = 0.0742	*R*1 = 0.1092, *wR*2 = 0.0693	*R*1 = 0.0443, *wR*2 = 0.0933
Largest diff. peak and hole, eA^{-3}	0.376, −0.210	0.523, −0.315	0.291, −0.194	0.205, −0.196	0.326, −0.246

Table 2. Selected bond lengths (pm), bond angles (°) and N···K$^+$ separation (pm) in salts **1**, **3**−**6** (for atom numbering see Figure 1−5); for comparison, the data of the corresponding TAS$^+$ salts of **2**,[7] **3**,[7] and **5**[8] are included

Salt	R−N2	N2−S1	S1−N1	R−N2−S1	N2−S1−N1	N1···K$^+$
1	147.4(3)	156.5(2)	147.2(2)	125.70(17)	126.55(12)	270.3(2)
2(TAS$^+$)[7]	147.4(2)	157.6(1)	149.0(1)	123.81(10)	125.82(7)	−
3	172.1(3)	154.9(3)	146.4(3)	123.99(19)	118.80(17)	292.0(3)[a]
3(TAS$^+$)[7]	171.7(3)	156.4(3)	146.7(2)	124.5(2)	121.3(2)	−
4	140.3(3)	159.1(2)	145.8(2)	126.31(15)	125.45(11)	272.6(2)
5	141.9(6)	157.0(4)	146.1(4)	127.2(4)	125.3(2)	270.7(5)
5(TAS$^+$)[8]	138.8(7)	160.3(5)	146.9(5)	126.0(4)	124.5(3)	−
6	−	148.4(3)	148.4(3)	−	129.9(2)	295.0(4)/293.9(4)

[a] N2···K$^+$ 295.6(3), S1···K$^+$ 339.81(12) pm.

same [RNSN]$^-$ anions, it can be seen that exchange of the cation affects the bond lengths and bond angles in the anion to some extent; however the differences are relatively small (Table 2).

The reason for the reorganization of the chemical bonding on going from the R−N=S=N−SiMe$_3$ precursors to the corresponding R−N$^-$−S≡N anions is not entirely clear.[7,8] It follows from a preliminary analysis of the calculations at the MP2/6-31+G* level of theory that this reorganization is driven to some extent by the reduction of the local symmetry at the S atom.[25,26]

The [NSN]$^{2-}$ dianion (salt **6**) is the genuine aza-analogue of sulfur dioxide O=S=O (and isoelectronic with ozone, O$_3$). As mentioned above, no structural characterization using X-ray crystallography has been reported in the literature. On the basis of vibrational spectra,[23] its C_{2v} symmetry was determined and confirmed independently by quantum chemical calculations at the RHF level of theory.[27]

In the gas phase, the structure of the O=S=O molecule was determined by microwave spectroscopy with sulfur−oxygen bond lengths of 143.1 pm and a OSO bond

angle of 119.3°.[28] Recently, the solid-state structure was also reported from a low temperature X-ray study [sulfur−oxygen bond length 142.97 (4) pm and OSO angle 117.5(1)°].[29]

In the crystal structure, the sulfur atom of the $[NSN]^{2-}$ dianion is situated very close to a crystallographic center of inversion and therefore the anion is disordered over two positions. The two independent S−N distances were refined with one common value and the calculations converged at 148.4(3) pm with a N−S−N angle of 129.9(2)°. Our theoretical calculations (Table 3) agree reasonably well with our experimental results.

Table 3. Bond lengths (pm) and bond angles (°) of the $[NSN]^{2-}$ anion from quantum chemical calculations

	RHF[a]	MP2[a]	B3LYP[a]	Exp.
(*d* S−N)	149.9	155.8	154.4	148.4(3)
(< N−S−N)	129.8	134.0	131.4	129.9(2)

[a] Basis set: 6−311+G*; for all methods NIMAG = 0.

Relative to O=S=O, in the $[NSN]^{2-}$ dianion, the bond lengths [148.4(3) pm] are elongated by ca. 5 pm and the bond angle [129.9(2)°] is widened by ca. 12 degrees (Table 2). This might reflect the electrostatic repulsion between the negatively charged N atoms. To the best of our knowledge, high level quantum chemical calculations on $[NSN]^{2-}$ are not reported in the literature. Earlier MNDO and HFS calculations,[27] not surprisingly, do not reproduce the experimentally observed geometry.

Previously, the $[RNSN]^-$ anions (R = *t*Bu, Me_3Si) and the $[NSN]^{2-}$ dianion (with Me_4N^+, nBu_4N^+ and TAS^+ as counterions) were characterized by multinuclear NMR spectroscopy (including nitrogen) in solution and in the solid state[7,30,31] (nitrogen NMR spectroscopy of binary sulfur-nitrogen anions, see ref.[32−34]). For $[RNSN]^-$, the high-field signal in the nitrogen (^{14}N and ^{15}N) NMR spectra can always be assigned to the internal (substituted) N atom and the low-field signal to the terminal (unsubstituted) N atom.

Table 4. Multinuclear NMR spectroscopic data (δ, ppm) for the salts **1**−**6**

R	^1H	^{13}C	^{14}N	^{39}K
1	3.55, 2.11, 1.93, 1.64	70.4, 57.5, 44.8, 37.6, 30.9	477, 310	−5.6
2	3.55, 1.20	70.5, 58.8, 31.1	485, 308	−5.3
3[a][b]	3.54, −0.16	70.5, 3.1	550, 286	−5.3
4	7.56, 7.10, 6.26, 3.54	150.9, 128.9, 123.1, 120.7, 71.0	512, 290	−6.1
5[c]	7.67, 6.82, 3.50	157.2, 147.3, 123.8, 114.7, 70.7	506.2[d], 285.1[d]	−5.4
6[e]	3.53	70.7	382	−4.0

[a] $\delta^{29}Si = -15.2$. [b] cf. Me_4N^+ salt: $\delta^1H = 3.24$ (Me_4N^+), −0.01; $\delta^{13}C = 56.0$ (Me_4N^+), 3.3; $\delta^{29}Si = -13.4$; $\delta^{14}N = 542, 294, 46$ (Me_4N^+). The salt was obtained from a 1:1 reaction of $(Me_3Si-N=)_2S$ with Me_4NF as large transparent orange-yellow scales (85%), m.p. (from MeCN) 140−141 °C (decomposition with gas evolution).[29] [c] $\delta^{19}F = 38.0$. [d] $\delta^{15}N$ ($\delta^{14}N = 507, 283$). [e] Me_4N^+ salt: $\delta^1H = 3.20$ (Me_4N^+); $\delta^{13}C = 55.9$ (Me_4N^+); $\delta^{14}N = 383, 46$ (Me_4N^+). The salt was obtained from a 1:2 reaction of $(Me_3Si-N=)_2S$ with Me_4NF as well-shaped orange-red prisms (90%), m.p. (from MeCN) 161−162 °C (decomposition with gas evolution).[29]

The multinuclear (^1H, ^{13}C, ^{14}N, ^{19}F, ^{29}Si, ^{39}K) NMR spectroscopic data for solutions of the salts **1**−**6** in acetonitrile are presented in Table 4. It follows from the Table 3 that on going from $[AlkNSN]^-$ (Alk = *t*Bu, 1-Ad) to $[ArNSN]^-$ (Ar = Ph, 4-FC_6H_4) (all four are in the *Z* configuration), the signal for the internal N atom shifts further high field, whereas the signal for the terminal N atom shifts in the opposite direction further low field. As a result, the $\Delta\delta^{14}N$ difference between magnetic shielding of the internal and terminal N atoms is larger in the $[ArNSN]^-$ than in the $[AlkNSN]^-$ anions.

The single ^{14}N NMR resonance for the $[NSN]^{2-}$ dianion is found between those of the terminal and the internal N atoms of the $[RNSN]^-$ anions (Table 3). The chemical shift is practically independent of the counterion (Me_4N^+, nBu_4N^+, TAS^+, $[K(18\text{-crown-6})]^+$).

Conclusion

$[K(18\text{-crown-6})]^+$ salts of the $[RNSN]^-$ anions (R = Alk, Ar), including that with R = Ph (the parent compound of the $[ArNSN]^-$ family), as well as of the $[NSN]^{2-}$ dianion, were prepared for the first time and structurally characterized by X-ray diffraction in the solid state and by multinuclear NMR spectroscopy (including nitrogen) in solution. The experimentally determined bond lengths confirm that the $[RNSN]^-$ anions are thiazylamides $R-N^--S\equiv N$ rather than sulfur diimides $R-N=S=N^-$. As observed for the corresponding TAS-salts, TAS^+RNSN^-, the substituent R occupies the electronically unfavorable E-position only in the Me_3Si derivative.[6−8] The present investigation shows that even bulky substituents and strong anion−cation interactions do not influence the preference of the alkyl and aryl substituents for the *Z*-position.

Relative to O=S=O, in the $[NSN]^{2-}$ dianion, which is the genuine aza-analogue of sulfur dioxide, the bond lengths are elongated and the bond angle is widened; this might reflect Coulombic repulsion between the N atoms. In the nitrogen NMR spectra, when going from $[AlkNSN]^-$ to $[ArNSN]^-$ the low-field signal of the terminal N atoms reveals further deshielding, whereas the high-field signal of internal N atoms display further shielding. The single ^{14}N NMR resonance for the $[NSN]^{2-}$ dianion is not influenced by the counterion.

Due to anion−cation interactions, the salts prepared are thermally very stable. Their stability and their good solubility in aprotic organic solvents (THF, MeCN) facilitates their use in synthetic chemistry as key intermediates for various inter- and intramolecular condensations. They can also be used as ligands for coordination compounds.

Experimental Section

Materials and Methods: The starting $R-N=S=N-SiMe_3$ and $(Me_3Si-N=)_2S$ compounds were synthesized as described previously.[11,13,35] *t*BuOK (Janssen Chimica) was sublimed in vacuo, 18-crown-6 (Aldrich) was used as received. Absolute MeCN, THF, Et_2O and *n*-pentane were prepared by standard methods. The multinuclear NMR spectra were measured using a Bruker DRX-500 spectrometer at frequencies of 500.13 (^{1}H), 125.76 (^{13}C), 36.13 (^{14}N), 50.68 (^{15}N), 470.59 (^{19}F), 99.36 (^{29}Si), and 23.34 (^{39}K) MHz for solutions in CD_3CN; the chemical shifts (Table 2) are referred to TMS (^{1}H, ^{13}C, ^{29}Si), NH_3 (l) (^{14}N, ^{15}N), C_6F_6 (^{19}F) and KCl (aq.) (^{39}K). The melting points were measured using a Gallencamp Melting Point Apparatus in sealed capillaries. For all salts melting was accompanied by decomposition with gas evolution.

Preparation of $[K(18\text{-crown-6})]^+[RNSN]^-$ (R = Ad (1), *t*Bu (2), Ph (4), 4-FC_6H_4 (5): Under dry argon, at −40 °C, a solution of the corresponding $R-N=S=N-SiMe_3$ (5 mmol) in THF (5 mL) was added dropwise to a stirred solution of $[K(18\text{-crown-6})]^+[t\text{BuO}]^-$ (1.88 g, 5 mmol) in THF (20 mL) (prepared from *t*BuOK (0.56 g, 5 mmol) and 18-crown-6 (1.32 g, 5 mmol) at −20 °C). After an additional 2 h at the same temperature, the solvent was removed under high vacuum. MeCN (20 mL) was redistilled onto the solid residue via a vacuum line at −196 °C. On warming to −40 °C, the red solution formed was filtered through a sintered glass frit, cooled again to −196 °C, and Et_2O (20 mL) was condensed onto it. The reaction vessel was placed into a cryostat at −35 °C for crystal growth. After 2 weeks, when mutual diffusion of the solvents ceased, the mother liquor was removed with a syringe under dry argon at −40 °C. The crystalline residue was washed with Et_2O and dried in vacuo at ambient temperature.

$[K(18\text{-crown-6})]^+[1\text{-AdNSN}]^-\cdot$MeCN (1): Large transparent orange-yellow prisms, 2.30 g (85%), m.p. 106−108 °C.

$[K(18\text{-crown-6})]^+[t\text{BuNSN}]^-$ (2): Large transparent orange-yellow crystals, 1.90 g (90%), m.p. 149−150 °C.

$[K(18\text{-crown-6})]^+[\text{PhNSN}]^-$ (4): Orange-red crystals, 1.58 g (72%), m.p. 110−112 °C.

$[K(18\text{-crown-6})]^+[4\text{-}FC_6H_4NSN]^-$ (5): Orange-brown crystals, 1.28 g (56%), m.p. 98−100 °C.

Preparation of $[K(18\text{-crown-6})]^+[Me_3SiNSN]^-$ (3) (a) and $\{[K(18\text{-crown-6})]^+\}_2[NSN]^{2-}$ (6) (b): Under dry argon, at −40 °C, a solution of $(Me_3Si-N=)_2S$ (1.03 g, 5 mmol) (a) or (0.50 g, 2.5 mmol) (b) in THF (5 mL) was added dropwise to a stirred solution of $[K(18\text{-crown-6})]^+[t\text{BuO}]^-$ (1.88 g, 5 mmol) inTHF (20 mL), prepared as described above. After an additional 2 h at the same temperature, the reaction solution was filtered through a sintered glass frit and *n*-pentane (20 mL) was condensed onto it via a vacuum line at −196 °C. For crystal growth, the reaction vessel was placed into a cryostat at −35 °C (a) or kept at 20 °C (b). After 2 weeks, the solvents were removed as described above, and the crystalline residue was washed with Et_2O and dried in vacuo at ambient temperature.

$[K(18\text{-crown-6})]^+[Me_3SiNSN]^-\cdot$THF (3): Orange-yellow crystals, 2.09 g (82%), m.p. 106−108 °C.

$\{[K(18\text{-crown-6})]^+\}_2[NSN]^{2-}$ (6): Large bronze-brown crystals (orange-yellow when freshly prepared; dark orange in transmitting light), 1.50 g (90%), m.p. 152−154 °C.

X-ray Crystallographic Study: The single-crystal X-ray structure determinations (Table 1) were carried out on a Stoe IPDS for **1**, **3**, **4**, and on a Siemens P4 diffractometer for **5** and **6**, using Mo-K_α (0.71073 Å) radiation with a graphite monochromator. Refinement based on F^2; $R1 = \|F_o| - |F_c\|/|F_o|$; $wR2 = \{[w(F_o^2 - F_c^2)^2/[w(F_o^2)^2]\}^{1/2}$. Programs used: SHELX-97[36] and DIAMOND.[37] The structures of **1** and **4** were refined as racemic twins. In the crystal packing of **6**, the anion and cation are both disordered. The single crystals were mounted on a thin glass fiber using KEL-F oil. The structures were solved by direct methods (SHELXS[36]). Subsequent least-squares refinements (SHELXL-97-2[36]) located the positions of the remaining atoms in the electron density maps. All non-H atoms were refined anisotropically.
CCDC-227222 (for **1**), -227223 (for **2**), -227224 (for **4**), -227225 (for **5**), -227226 (for **6**) contain the supplementary crystallographic data for this paper. These data can be obtained free of charge at www.ccdc.cam.ac.uk/conts/retrieving.html [or from the Cambridge Crystallographic Data Centre, 12 Union Road, Cambridge CB2 1EZ, UK; Fax: (internat.) + 44-1223-336-033; E-mail: deposit@ccdc.cam.ac.uk].

Quantum Chemical Calculations: Quantum chemical calculations were performed with the Gaussian 98 set of programs.[38]

Acknowledgments

The authors are grateful to Dr. Paul G. Watson for NMR spectroscopic measurements on the Me_4N^+ salts, and to Mr. Peter Brackmann for technical assistance with the X-ray diffraction measurements. The joint financial support of this work by the DFG, Germany (Project 436 RUS 113/486/0−2 R), and the RFBR, Russia (Project 02−03−04001), is gratefully acknowledged. A.Z. is also grateful to the RFBR for financial support within Project 02−03−32794.

[1] O. Glemser, R. Mews, *Angew. Chem. Int. Ed. Engl.* **1980**, *19*, 883−899.
[2] G. Hartmann, R. Mews, G. M. Sheldrick, R. Anderskewitz, M. Niemeyer, H. J. Emeleus, H. Oberhammer, *J. Fluorine Chem.* **1986**, *34*, 46−58.
[3] R. Maggiulli, E. Lork, U. Behrens, K. Burger, R. Mews, *J. Fluorine Chem.* **2000**, *102*, 337−343.
[4] T. Yoshimura, *Rev. Heteroatom Chem.* **2000**, *22*, 101−120.
[5] T. Fujii, A. Itoh, K. Hamata, T. Yoshimura, *Tetrahedron Lett.* **2001**, *42*, 5041−5043.
[6] A. V. Zibarev, E. Lork, R. Mews, *Chem. Commun.* **1998**, 991−992.
[7] T. Borrmann, A. V. Zibarev, E. Lork, G. Knitter, S.-J. Chen, P. G. Watson, E. Cutin, M. M. Shakirov, W.-D. Stohrer, R. Mews, *Inorg. Chem.* **2000**, *39*, 3999−4005.
[8] T. Borrmann, E. Lork, R. Mews, W.-D. Stohrer, P. G. Watson, A. V. Zibarev, *Chem. Eur. J.* **2001**, *7*, 3504−3510.
[9] A. V. Zibarev, A. O. Miller, *J. Fluorine Chem.* **1990**, *50*, 359−363.
[10] A. V. Zibarev, Y. V. Gatilov, A. O. Miller, *Polyhedron* **1992**, *11*, 1137−1141.
[11] I. Y Bagryanskaya, Y. V. Gatilov, A. O. Miller, M. M. Shakirov, A. V. Zibarev, *Heteroatom Chem.* **1994**, *5*, 561−565.
[12] E. Lork, R. Mews, M. M. Shakirov, P. G. Watson, A. V. Zibarev, *Eur. J. Inorg. Chem.* **2001**, 2123−2134.
[13] E. Lork, R. Mews, M. M. Shakirov, P. G. Watson, A. V. Zibarev, *J. Fluorine Chem.* **2002**, *115*, 165−168.
[14] A. Y. Makarov, I. Y. Bagryanskaya, F. Blockhuys, C. Van Alsenoy, Y. V. Gatilov, V. V. Knyazev, A. M. Maksimov, T. V. Mikhalina, V. E. Platonov, M. M. Shakirov, A. V. Zibarev, *Eur. J. Inorg. Chem.* **2003**, 77−88.

[15] M. Herberhold, S. Gerstmann, B. Wrackmeyer, *Phosphorus Sulfur Silicon Relat. Elem.* **1992**, *66*, 273−283.
[16] M. Herberhold, S. Gerstmann, B. Wrackmeyer, *Phosphorus Sulfur Silicon Relat. Elem.* **1996**, *113*, 89−106 (and references cited therein).
[17] D. Haenssgen, R. Boss, *Z. Anorg. Allg. Chem.* **1981**, *437*, 80−84.
[18] M. Herberhold, W. Ehrenreich, K. Guldner, *Chem. Ber.* **1984**, *117*, 1999−2005.
[19] A. Gieren, H. Betz, T. Huebner, V. Lamm, M. Herberhold, K. Guldner, *Z. Anorg. Allg. Chem.* **1984**, *513*, 160−174.
[20] N. P. C. Walker, M. B. Hursthouse, C. P. Warrens, J. D. Woollins, *J. Chem. Soc., Chem. Commun.* **1985**, 227−228.
[21] A. Modelli, V. Venuti, F. Scagnolari, D. Jones, *Chem. Phys. Lett.* **2001**, *346*, 492−496.
[22] O. A. Dyachenko, O. N. Kazheva, personal communication **2001**.
[23] M. Herberhold, W. Ehrenreich, *Angew. Chem.* **1982**, *94*, 637−638; *Angew. Chem. Int. Ed. Engl.* **1982**, *21*, 633−63: *Angew. Chem. Suppl.* **1982**, 1346.
[24] M. Herberhold, W. Ehrenreich, W. Buehlmeyer, K. Guldner, *Chem. Ber.* **1986**, *119*, 1424−1428.
[25] L. N. Shchegoleva, personal communication, **2002**.
[26] Y V. Gatilov, R. Mews, L. N. Shchegoleva, A. V. Zibarev, work in progress.
[27] M. Conti, M. Trsic, W. G. Laidlaw, *Inorg. Chem.* **1986**, *25*, 254−256.
[28] Y. Morino, M. Tanimoto, S. Saito, *Acta Chim. Scand., Ser. A* **1988**, *42*, 346−351.
[29] J. Buschmann, W. Steudel, personal communication.
[30] B. Wrackmeyer, S. Gerstmann, M. Herberhold, G. A. Webb, H. Kirosu, *Magn. Reson. Chem.* **1994**, *32*, 492−495.
[31] E. Lork, R. Mews, P. G. Watson, A. V. Zibarev, unpublished results, **2000**.
[32] T. Chivers, K. J. Schmidt, *Can. J. Chem.* **1992**, *70*, 710−718.
[33] T. Chivers, D. D. McIntyre, K. J. Schmidt, H. J. Vogel, *J. Chem. Soc., Chem. Commun.* **1990**, 1341−1342.
[34] T. Chivers, K. J. Schmidt, *J. Chem. Soc., Chem. Commun.* **1990**, 1342−1344.
[35] A. V. Zibarev, A. O. Miller, Y. V. Gatilov, G. G. Furin, *Heteroatom Chem.* **1990**, *1*, 443−453.
[36] G. M. Sheldrick, *SHELX-97 − Programs for Crystal Structure Analysis (Release 97−2)*, Institute for Inorganic Chemistry, University of Göttingen, Göttingen, Germany, **1997**.
[37] *DIAMOND − Visual Structure Information System*, Crystal Impact, Bonn, Germany.
[38] M. J. Frisch, G. W. Trucks, H. B. Schlegel, G. E. Scuseria, M. A. Robb, J. R. Cheeseman, V. G. Zakrzewski, J. A. Montgomery, Jr., R. E. Stratmann, J. C. Burant, S. Dapprich, J. M. Millam, A. D. Daniels, K. N. Kudin, M. C. Strain, O. Farkas, J. Tomasi, V. Barone, M. Cossi, R. Cammi, B. Mennucci, C. Pomelli, C. Adamo, S. Clifford, J. Ochterski, G. A. Petersson, P. Y. Ayala, Q. Cui, K. Morokuma, D. K. Malick, A. D. Rabuck, K. Raghavachari, J. B. Foresman, J. Cioslowski, J. V. Ortiz, A. G. Baboul, B. B. Stefanov, G. Liu, A. Liashenko, P. Piskorz, I. Komaromi, R. Gomperts, R. L. Martin, D. J. Fox, T. Keith, M. A. Al-Laham, C. Y. Peng, A. Nanayakkara, C. Gonzalez, M. Challacombe, P. M. W. Gill, B. Johnson, W. Chen, M. W. Wong, J. L. Andres, C. Gonzalez, M. Head-Gordon, E. S. Replogle, J. A. Pople, *Gaussian 98, Revision A.7*, Gaussian Inc., Pittsburgh PA, **1998**.

Received December 19, 2003
Early View Article
Published Online April 26, 2004

